

Document downloaded from:

<http://hdl.handle.net/10251/121742>

This paper must be cited as:

Bayad, H.; Elmanouni, A.; Marí, B.; Khattak, YH.; Ullah, S.; Baig, F. (2018). Influence of P+ - ZnTe back surface contact on photovoltaic performance of ZnTe based solar cells. *Optical and Quantum Electronics*. 50(6):1-14. <https://doi.org/10.1007/s11082-018-1530-0>



The final publication is available at

<http://doi.org/10.1007/s11082-018-1530-0>

Copyright Springer-Verlag

Additional Information

Influence of P⁺-ZnTe back surface contact on photovoltaic performance of ZnTe based solar cells

Hamza Bayad^{1,2}, Ahmed El Manouni², Bernabé Mari¹, Yousaf H. Khattak^{1,3}, Shafi Ullah¹, Faisal Baig^{1,3}

¹ETS de Ingeniería de Diseño, Departament de Física Aplicada, Universitat Politècnica de València, Camí de Vera (SPAIN)

²Laboratoire LPAMM, Département de physique, Université Hassan II, Faculté des Sciences et Techniques, BP 145 Mohammedia (Morocco)

³Department of Electrical Engineering, Federal Urdu University of Arts, Science and Technology Islamabad, (PAKISTAN)
ha.ba.om@gmail.com, elmanouni123@gmail.com, bmari@fis.upv.es, yousaf.hameedk@gmail.com,

shafi399@yahoo.com, engr.fsl.baig@gmail.com

Abstract— In order to improve photovoltaic performance of solar cells based on ZnTe thin films two device structures have been proposed and its photovoltaic parameters have been numerically simulated using Solar Cell Capacitance Simulator software. The first one is the ZnO/CdS/ZnTe conventional structure and the second one is the ZnO/CdS/ZnTe/P⁺-ZnTe structure with a P⁺-ZnTe layer inserted at the back surface of ZnTe active layer to produce a back surface field effect which could reduce back carrier recombination and thus increase the photovoltaic conversion efficiency of cells. The effect of ZnO, CdS and ZnTe layer thicknesses and the P⁺-ZnTe added layer and its thickness have been optimized for producing maximum working parameters such as: open-circuit voltage V_{oc} , short-circuit current density J_{sc} , fill factor FF, photovoltaic conversion efficiency η . The solar cell with ZnTe/P⁺-ZnTe junction showed remarkably higher conversion efficiency over the conventional solar cell based on ZnTe layer and the conversion efficiency of the ZnO/CdS/ZnTe/P⁺-ZnTe solar cell was found to be dependent on ZnTe and P⁺-ZnTe layer thicknesses. The optimization of ZnTe, CdS and ZnTe layers and the inserting of P⁺-ZnTe back surface layer results in an enhancement of the energy conversion efficiency since its maximum has increased from 10% for ZnO, CdS and ZnTe layer thicknesses of 0.05, 0.08 and 2 μm , respectively to 13.37% when ZnO, CdS, ZnTe and P⁺-ZnTe layer thicknesses are closed to 0.03, 0.03, 0.5 and 0.1 μm , respectively. Furthermore, the highest calculated output parameters have been $J_{sc} = 9.35 \text{ mA/cm}^2$, $V_{oc} = 1.81 \text{ V}$, $\eta = 13.37\%$ and $FF = 79.05\%$ achieved with ZnO, CdS, ZnTe, and P⁺-ZnTe layer thicknesses about 0.03, 0.03, 0.5 and 0.1 μm , respectively. Finally, the spectral response in the long-wavelength region for ZnO/CdS/ZnTe solar cells has decreased at the increase of back surface recombination velocity. However, it has exhibited a red shift and showed no dependence of back surface recombination velocity for ZnO/CdS/ZnTe/P⁺-ZnTe solar cells.

Keywords: ZnTe, numerical simulation, back surface field, solar cells, photovoltaic performance.

I. INTRODUCTION

Numerical simulation methods have been indispensable tools for the design of any kind of efficient solar cells. They have contributed greatly to our understanding of optical and electrical properties operation of these cells and are necessary for future cell improvements [1–3]. To push cell efficiency toward the Shockley-Queisser limit several simulation programs, such as PC-1D, AMPS-1D, NSSP, ADEPT-F, AFORS-HET, ASPIN, ASA and SCAP, have been developed for the optimization of designs and for the comparison of competing design proposals. In the case of solar cells, numerical solution techniques allow the inclusion of important physical effects which otherwise could not be considered. These may include spatially dependent materials such as doping dependent mobility, lifetime, and band-gaps. Typically, inclusion of any one of these effects will prevent a closed form solution to the problem. The use of numerical techniques allows solutions to be obtained even when all of the above effects are included simultaneously [4, 5].

ZnTe semiconductor has been of interest for solar cells owing to its wide bandgap of 2.23-2.29 eV at room temperature [6], high electronic affinity of 3.73 eV [7], high absorption coefficient of 10^5 cm^{-1} [8] and high potential conversion efficiency with low-cost manufacturability and concern over environmental effects. It can be a potential candidate to substitute for the widely used CdTe semiconductor as an absorber in solar cells which is very toxic because of the cadmium element. ZnTe crystallizes in zinc-blend crystal structure and its conductivity is p-type doping due to native defect structure, such as zinc vacancy [9-11] in contrast with other wide-bandgap semiconductors such as ZnO, materials typically n-type and difficult to convert to p-type conduction.

The present work constitutes a continuity of our previous work concerning modeling and the optimization of solar cells based on ZnTe thin films by means of Solar Capacitance Simulator software SCAPS-1D [12]. It aims improving photovoltaic output characteristics of ZnTe based solar cells by optimizing its different layers and inserting of a P⁺-ZnTe layer at the back surface of ZnTe absorber in order to inhibit recombination loss at the back contact of cells. This P⁺-ZnTe layer would act as a back surface field (BSF) which could rappel the photogenerated carriers at ZnTe/P⁺-ZnTe interface and thus would decrease the loss of carriers at the back contact and therefore would increase the collected photocurrent and power conversion efficiency (PCE).

The main purpose of this work has been modeling solar cells based on ZnTe material with ZnO/CdS/ZnTe and ZnO/CdS/ZnTe/P⁺-ZnTe structures and studying the BSF effect due to the P⁺-ZnTe layer. The photovoltaic parameters of the proposed devices based on ZnTe thin films have been calculated and optimized. Finally, a comparative study of the photovoltaic performance of both solar cell structures has been carried out.

II. METHODOLOGY AND SIMULATION CONDITIONS

SCAPS is 1-dimensional simulation program used for simulate the electrical characteristics of thin-film heterojunction solar cells by solving the basic semiconductor equations under steady state conditions [13, 14]. SCAPS has been used in this work to simulate ZnTe based solar cells with and without P⁺-ZnTe back surface layer. Two solar devices have been simulated: the first one is the ZnO/CdS/ZnTe structure as developed in our previous work [12] and the second is constituted with four input layers and its structure is ZnO/CdS/ZnTe/P⁺-ZnTe as shown in Figure 1. The p-ZnTe film is used as an active layer (absorber), n-CdS as a buffer layer, ZnO as a window film and P⁺-ZnTe material as a back surface layer inserted at the back surface of ZnTe absorber. Furthermore, aluminum and platinum (Pt) metals are used as front and back contacts, respectively. The device design of the optimized ZnO/CdS/ZnTe/P⁺-ZnTe is shown in the substrate configuration and the illuminated side is the ZnO window (Fig 1).

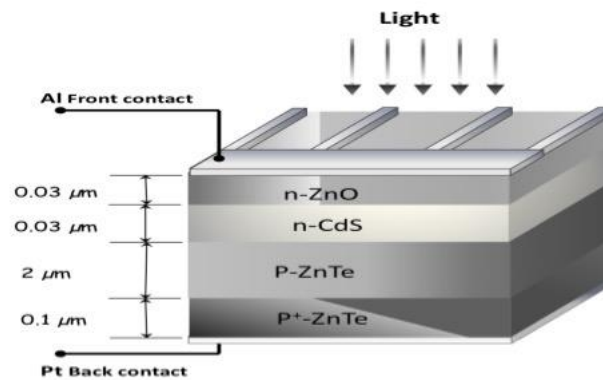


Figure 1: Solar device structure based on ZnTe thin film with P⁺-ZnTe back surface contact layer.

To simulate photovoltaic parameters of the proposal ZnO/CdS/ZnTe and ZnO/CdS/ZnTe/P⁺-ZnTe solar cells, SCAPS resolves three well known governing semiconductor equations: Poisson's equation and electron and hole continuity equations. The numerical resolution is performed on three coupled partial differential equations for the electrostatic potentials electron and hole concentration as function of position. Numerical calculations via SCAPS program require electrical and physical properties relative to all layers of the devices as well as the deep bulk defects and interface defect recombination (radiative and non-radiative recombinations). Defects in both CdS and ZnO layers have been assumed as neutral deep levels with Gaussian distribution while deep defects of both ZnTe absorber and P⁺-ZnTe back surface layer have been considered as uniform acceptor single levels of energy 0.51 and 0.60 eV respect to valence band edge E_V due to the zinc vacancy defect [15]. All optical and electrical parameters for simulation are given in table I. To optimize photovoltaic performance of the proposed devices the thicknesses of ZnTe, CdS and ZnO films and P⁺-ZnTe back surface layer have been varied. Simulation calculations were carried out under standard illumination AM1.5. The temperature of the simulated devices has been maintained at 300 K.

TABLE I: BASIC PARAMETERS USED IN SIMULATION OF ZnTe BASED SOLAR CELLS [12, 15-18].

Contact parameters	Front contact (Al)		Back contact(Pt)	
Work function Φ (eV)	4.45		5.93	
Surface recombination velocity of electrons S_e (cm/s)	10^7		10^7	
Surface recombination velocity of holes S_h (cm/s)	10^7		10^7	
Reflectivity R_f	0.05		0.8	
Layer properties				
	P+-ZnTe (BSF)	P-ZnTe (absorber)	CdS (n type)	ZnO (TCO)
Thickness (μm)	0.1-8	2	0.01-0.09	0.001-0.06
Band gap (eV)	2.19	2.19	2.43	3.37
Electron affinity (eV)	3.73	3.73	4.0	4.45
Dielectric constant	10.3	10.3	9.35	9.00
CB effective density of state for electron (cm^{-3}) N_c	1.176×10^{18}	1.176×10^{18}	1.758×10^{18}	2.949×10^{18}
VB effective density of states (cm^{-3}) N_v	1.166×10^{19}	1.166×10^{19}	1.469×10^{19}	1.137×10^{19}
Electron thermal velocity (cm/s)	3.24×10^7	3.24×10^7	2.83×10^7	2.38×10^7
Hole thermal velocity (cm/s)	1.51×10^7	1.51×10^7	1.39×10^7	1.52×10^7
Electron mobility (cm^2/Vs) à 300K	330	330	100	100
Hole mobility (cm^2/Vs) à 300K	80	80	25	25
Defect layer properties				
Energy defect level respect to valence band edge E_V (eV)	0.51 0.60	0.51 0.60	1.2	1.65
Shallow donor density N_D (cm^{-3})	0	0	1.0×10^{18}	1.0×10^{18}
Shallow acceptor density N_A (cm^{-3})	1.0×10^{22}	2.16×10^{19}	0	1
Thermal capture cross section of electron (cm^{-2})	1.0×10^{-15}	1.0×10^{-15}	1.0×10^{-15}	1.0×10^{-15}
Thermal capture cross section of hole (cm^{-2})	1.0×10^{-15}	1.0×10^{-15}	1.0×10^{-15}	1.0×10^{-15}
Optical capture cross section of electron (cm^{-2})	1.0×10^{-12} 1.0×10^{-12}	1.0×10^{-12} 1.0×10^{-12}	1.0×10^{-13}	1.0×10^{-12}
Optical capture cross section of hole (cm^{-2})	1.0×10^{-15} 1.0×10^{-15}	1.0×10^{-15} 1.0×10^{-15}	1.0×10^{-13}	1.0×10^{-12}

III. RESULTS AND DISCUSSION

1) Analyse of photovoltaic performance of CdS/ZnTe solar cells

In this part, numerical analysis of photovoltaic output parameters of CdS/ZnTe solar cells as regard to ZnO, CdS, ZnTe layer thicknesses is performed and the effect of back surface recombination velocity is pointed out.

a) Energy band diagram

The energy band diagram of the conventional ZnO/CdS/ZnTe solar cell is shown in Figure 2. The diagram was generated by SCAPS program in the dark at zero bias and the energy levels are shown with respect to the Fermi level which is set to 0 eV. The diagram is plotted for ZnTe absorber layer, CdS buffer and ZnO window thicknesses of about 2, 0.03, 0.03 μm respectively. It can be noted that n type and p-type regions and the associated valence band (VB) and conduction band (CB) edges and the interfaces and their positions are clearly shown in the Figure. It is observed also the presence of a depletion zone at the CdS/ZnTe interface. Furthermore there is no Schottky barrier at the ZnTe/metal interface which could be contributed to recombination losses and then would reduce photovoltaic performance.

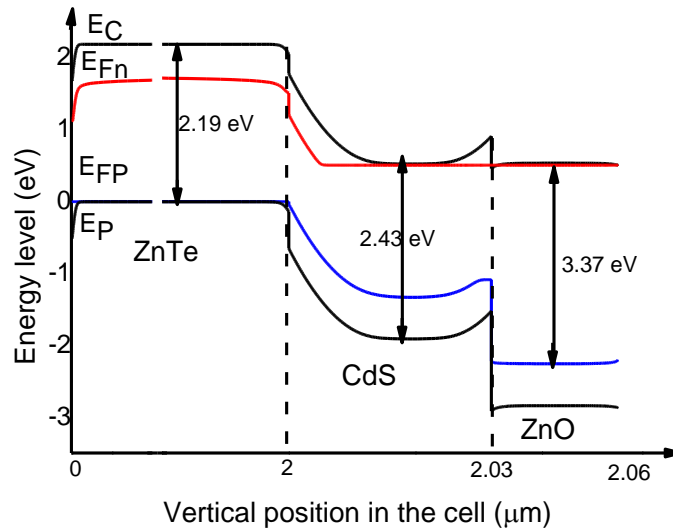


Figure 2: Schematic energy band diagram of the ZnO/CdS/ZnTe solar cell generated by SCAPS software at the dark and zero bias voltage.

b) Photovoltaic characteristics.

In order to confirm the necessity of reducing ZnTe active layer thickness to 2 μm in ZnO/CdS/ZnTe solar cell as found previously [12] total carrier generation rate as function of the position within ZnTe absorber has been calculated and plotted in Figure 3. From this figure it is observed that the carrier generation rate is around $2.25 \cdot 10^{21} \text{ cm}^{-3} \cdot \text{s}^{-1}$ near the CdS/ZnTe interface and then decreases drastically to $3.58 \cdot 10^{19} \text{ cm}^{-3} \cdot \text{s}^{-1}$ (by a factor of 0.01) within just 2 μm of ZnTe layer thickness and remains constant

for ZnTe thickness varying up to 8 μm . It results in that the optimal ZnTe absorber thickness can be 2 μm since the carriers have a little effect on the current when ZnTe thickness is higher than 2 μm .

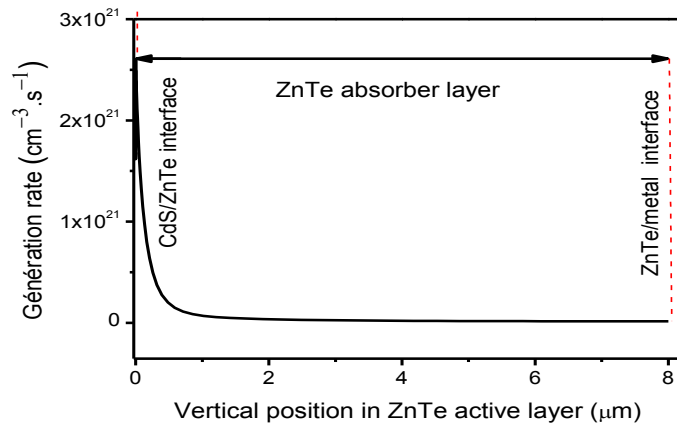


Figure 3: Total carrier generation rate in ZnO/CdS/ZnTe solar cell.

It is well known that window and buffer thicknesses affect photovoltaic performance of solar cells. So it is important to study the effect of CdS and ZnO layer thicknesses on the output parameters of the modeled ZnO/CdS/ZnTe solar cell. Numerical calculations for optimizing ZnO and CdS layer thicknesses have been developed and the obtained results are shown in Figure 4. From these results the optimal thickness of ZnO and CdS layers can be considered as 0.03 μm for each layer.

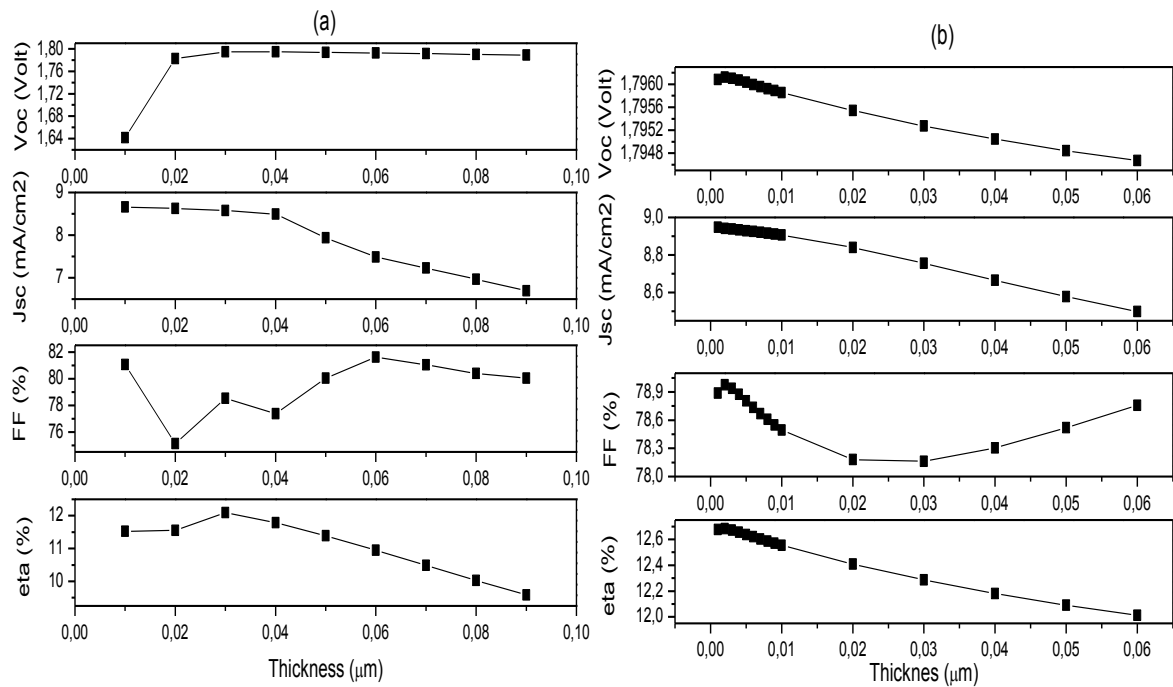


Figure 4: Photovoltaic performance of ZnO/CdS/ZnTe conventional solar cell as function of (a) CdS and (b) ZnO layer thicknesses.

The optimal characteristics of conventional ZnO/CdS/ZnTe solar cells are presented in table II. They have been obtained for ZnTe, ZnO and CdS optimal thicknesses of 2, 0.03, 0.03 μm , respectively; the calculated output parameters of ZnO/CdS/ZnTe solar cells without optimization of ZnO and CdS layer are given for comparison. It can be seen that optimizing ZnO and CdS layers results in an increase of the power conversion efficiency (PCE) from 10 to 12.28 %.

TABLE II: OPTIMAL OUTPUT PARAMETERS OF ZNTE BASED SOLAR CELLS.

Solar cell	Voc (Volt)	Jsc (mA/cm ²)	FF (%)	PCE (%)
ZnO/CdS/ZnTe [12]	1.81	7.01	78.84	10
ZnO/CdS/ZnTe after optimization of ZnO and CdS layers	1.795	8.75	78.16	12.28

In addition to the optimization of ZnO, CdS and ZnTe layers, the effect of the back surface recombination rate can be study in order to see its effect on photovoltaic performance of the ZnTe solar cells. In this sense, Figure 5 shows the variation of photovoltaic output parameters as function of the back surface recombination velocity. From this figure, it is shown that as the back surface recombination velocity increased, the photovoltaic characteristics decreased drastically. The maximum output parameters could be obtained when the recombination rate is lower than 10^4 cm/s. The decrease of photovoltaic characteristics in the case of conventional CdS/ZnTe solar cells is due to the back surface recombination losses that occur at the ZnTe/metal interface. Therefore, a new configuration could be proposed to inhibit the possible recombination losses at the back contact for thinner ZnTe absorber: keeping the conventional structure with inserting an optimal P+-ZnTe wide band gap material layer at the back surface of the ZnTe active layer.

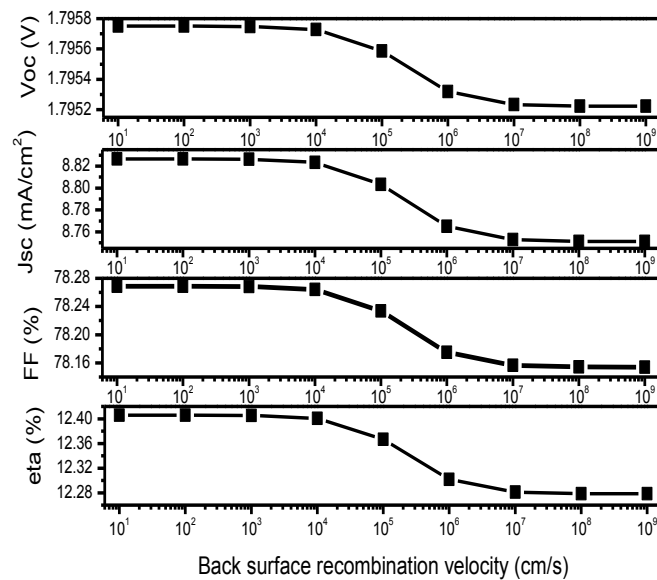


Figure 5: Effect of back surface recombination velocity on photovoltaic performance of ZnO/CdS/ZnTe solar cells for ZnTe, CdS and ZnO thicknesses of 2, 0.03 and 0.03 μm .

2) *Analyse of photovoltaic performance of CdS/ZnTe/P⁺-ZnTe solar cells*

To reduce the recombination losses at the back contact of ZnTe thin film based solar cells, a wide band-gap material such as P⁺-ZnTe semiconductor is inserted at the back surface of the ZnTe absorber layer. This material would act similarly to a BSF to repel the carriers at the ZnTe/P⁺-ZnTe heterojunction and thus would decrease the loss of carriers at the back contact. In numerical analysis, all input parameters are similar to those performed for the conventional ZnTe based solar cells, except the thickness of P⁺-ZnTe layer which has been varied from 0.1 to 8 μm and the shallow acceptor density which has closed to $1.0 \times 10^{22} \text{ cm}^{-3}$.

a) *Energy band diagram*

Figure 6 shows the energy band diagram generated by SCAPS for the ZnO/CdS/ZnTe/P⁺-ZnTe solar cell at zero bias in the dark with various positions within the cell layers. The band diagram is plotted for ZnTe, CdS, ZnO and P⁺-ZnTe layer thickness of 2, 0.03, 0.03 and 0.1 μm , respectively. Also, the energy levels are shown with respect to the Fermi level, which is set to 0 eV in the band diagram. In comparison with the energy band diagram of the conventional ZnO/CdS/ZnTe solar cell presented in Figure 2, a new barrier with height of about 0.195 eV is observed at the ZnTe/P⁺-ZnTe interface. This barrier would decrease carrier recombination losses at the back contact and could allow better collection of photogenerated carriers.

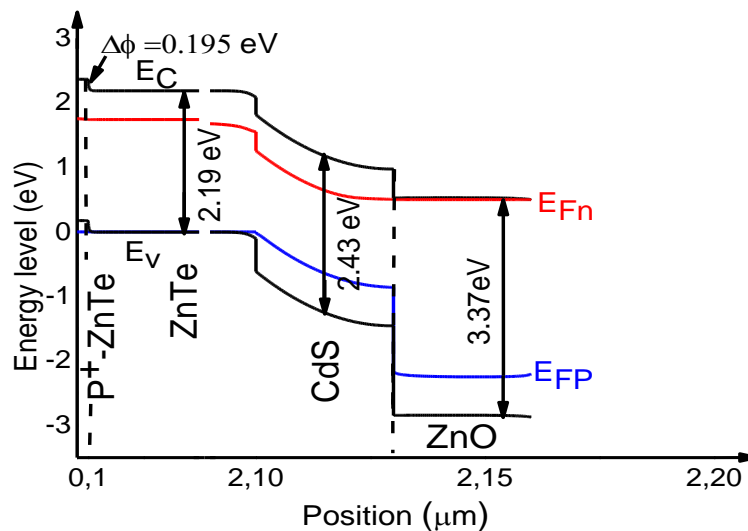


Figure 6: Schematic energy band diagram of ZnO/CdS/ZnTe/P⁺-ZnTe solar cell generated by SCAPS software at the dark and zero bias voltage.

b) *Photovoltaic characteristics of the ZnTe solar cell with P⁺-ZnTe back surface layer:*

Including parameter settings of P⁺-ZnTe layer, numerical calculations of photovoltaic characteristics on ZnO/CdS/ZnTe/P⁺-ZnTe solar cells have been carried out to determine the effect of P⁺-ZnTe layer. In this sense the effect of recombination rate on main output parameters has been performed and plotted

in Figure 7. The calculated photovoltaic parameters in the case of ZnO/CdS/ZnTe device are shown for comparison. In contrast with conventional ZnO/CdS/ZnTe solar cells, the characteristics of ZnO/CdS/ZnTe/P⁺-ZnTe solar cells showed no dependence on the back surface recombination rate. Also when the back surface recombination is higher than 10⁴ cm/s the characteristics for ZnO/CdS/ZnTe/P⁺-ZnTe cells became higher than those of ZnO/CdS/ZnTe devices. This indicates that the P⁺-ZnTe layer inserted at the back surface of ZnTe absorber film has favored the migration of photogenerated carriers towards the CdS/ZnTe interface for to be collected instead of recombining at the back contact of the cell. Thus, the carrier back recombination process is inhibited and a better carrier collection can be obtained.

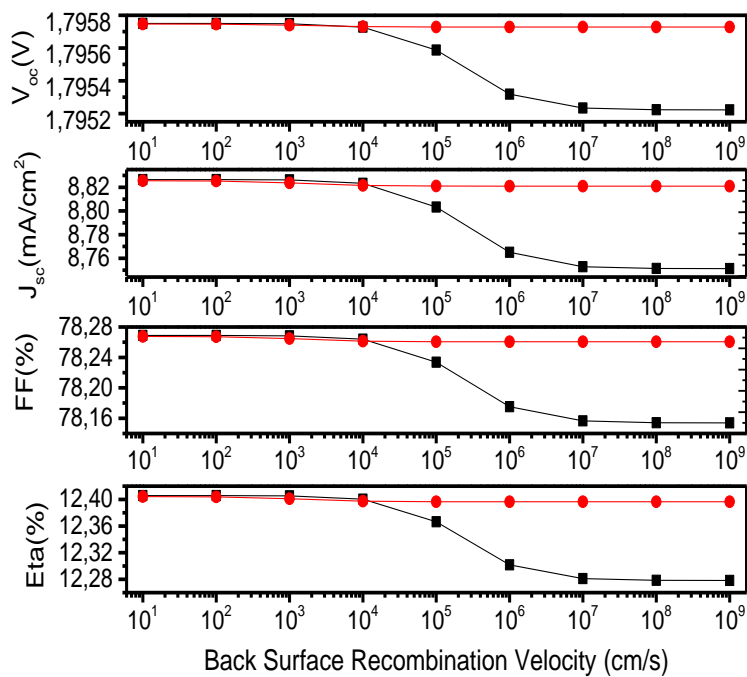


Figure 7: Comparison of the effect of back surface recombination velocity on the ZnO/CdS/ZnTe (black curve) and ZnO/CdS/ZnTe/P⁺-ZnTe (red curve) solar cells for ZnTe and P⁺-ZnTe layers of 2 and 0.1 μm respectively.

The effect of P⁺-ZnTe layer thickness on output parameters of ZnO/CdS/ZnTe/P⁺-ZnTe solar cells is shown in Figure 8. It is observed that as the P⁺-ZnTe layer thickness has increased from 0.1 to 8 μm the characteristics have decreased drastically. Thus the optimal thickness of P⁺-ZnTe layer will be fixed to 0.1 μm.

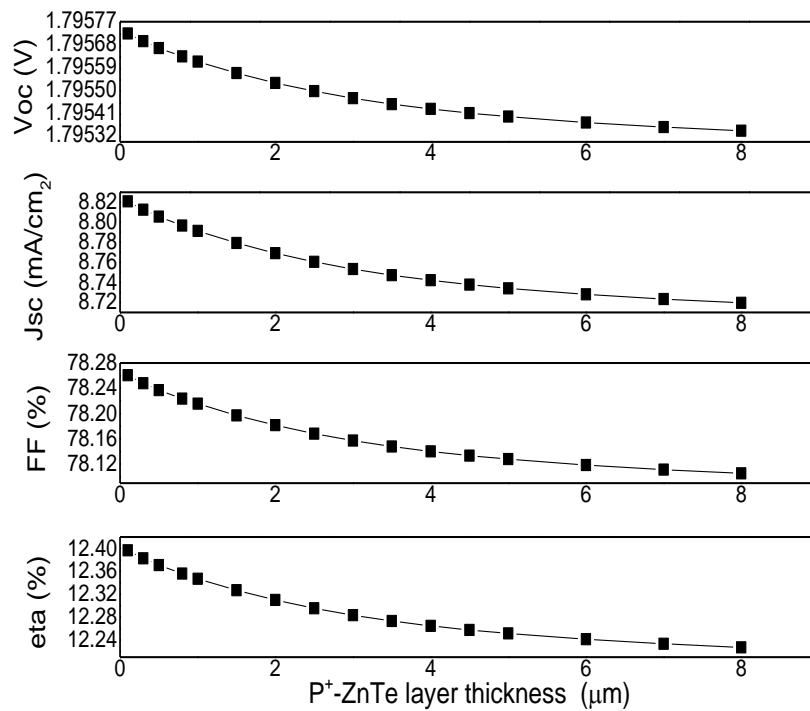


Figure 8: Photovoltaic performance of ZnO/CdS/ZnTe/P⁺-ZnTe solar cell as function of P⁺-ZnTe back surface layer thickness.

By comparing the obtained results of CdS/ZnTe and CdS/ZnTe/P⁺-ZnTe solar cells, one can observe that the solar cells with ZnTe/P⁺-ZnTe junction showed remarkably higher conversion efficiency over the conventional solar cell based on ZnTe layer. Indeed the conversion efficiency has increased from 10 % [12] for ZnO/CdS/ZnTe solar cell with ZnO, CdS and ZnTe layer thicknesses of 0.05, 0.08 and 2 μm respectively to 12.28 % for ZnO/CdS/ZnTe solar cell with ZnO, CdS and ZnTe layer thicknesses optimized to 0.03, 0.03 and 2 μm respectively and to 12.40 % for ZnO/CdS/ZnTe/P⁺-ZnTe device with ZnO, CdS, ZnTe and P⁺-ZnTe layer thicknesses closed to 0.03, 0.03, 2 and 0.1 μm respectively. This increase of energy conversion efficiency is due on one hand to the optimization of ZnO and CdS layers and to the insertion of P⁺-ZnTe film at the back surface of ZnTe active layer which has contributed to inhibit the back recombination of photogenerated carriers on the other hand.

The influence of ZnTe absorber thickness on photovoltaic performance of ZnTe based solar cells with and without P⁺-ZnTe back surface layer has been performed. Numerical calculations on the both solar cells have been carried out and the obtained results are shown in Figure 9. It is observed that all output parameters of the solar cell with ZnTe/P⁺-ZnTe junction are higher than those of the conventional ZnTe based device as ZnTe absorber thickness is lower than 2 μm, while they became equal and constant for ZnTe absorber thickness higher than 2 μm. From this analysis, the back surface field BSF is clearly carried out when ZnTe thickness is lower than 2 μm. Furthermore, contrary to the ZnO/CdS/ZnTe device the open-circuit voltage V_{oc} has showed an expected increase with the decrease of the ZnTe absorber

layer thickness for ZnO/CdS/ZnTe/P⁺-ZnTe solar cell. Also it is noted that the J_{sc}, FF and η parameters increased as ZnTe thickness increased up to 0.5 μm, reached a maximum when ZnTe thickness is equal to 0.5 μm and then decreased for ZnTe thickness varying from 0.5 to 1.5 μm before to became constant for ZnTe thickness varying from 1.5 to 8 μm. From this analysis, the optimal ZnTe thickness can be considered as 0.5 μm and the corresponding characteristics are V_{oc}=1.81 V, J_{sc}=9.35 mA/cm², FF=79.05 % and η=13.37 % obtained for ZnO, CdS, ZnTe and P⁺-ZnTe layer thicknesses of 0.03, 0.03, 0.5 and 0.1 μm, respectively. One can observe that the ZnTe optimal absorber thickness has changed from 2 to 0.5 μm when a P⁺-ZnTe back surface layer was added in ZnTe based solar cells. Thus an important reduction of absorber thickness can be realized and an improvement of photovoltaic performance of ZnTe based solar cells can be obtained simultaneously.

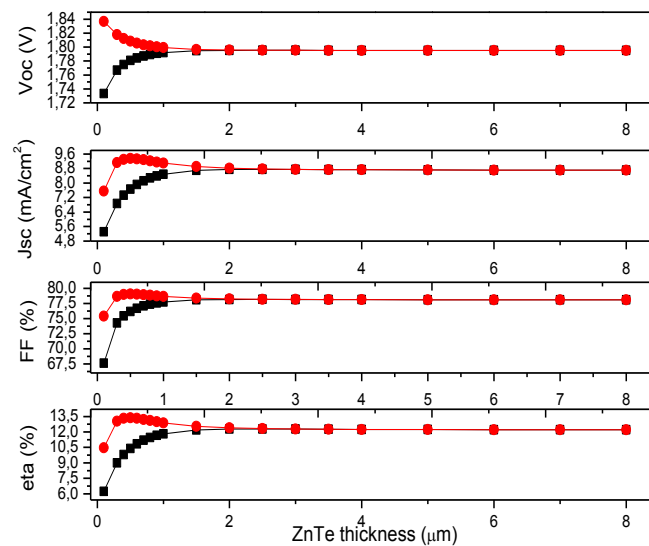


Figure 9: Photovoltaic output parameters as function of ZnTe absorber thickness for ZnO/CdS/ZnTe (black curve) and ZnO/CdS/ZnTe/P⁺-ZnTe (red curve) solar cells (ZnO, CdS and P⁺-ZnTe thicknesses are fixed to 0.03, 0.03 and 0.1 μm, respectively).

The optimal characteristics of both ZnO/CdS/ZnTe and ZnO/CdS/ZnTe/P⁺-ZnTe solar cells are presented in table III. It is observed that after optimizing ZnTe, CdS, ZnO and P⁺-ZnTe layers the energy conversion efficiency has increased from 10 to 13.37 %.

TABLE III: OPTIMAL PHOTOVOLTAIC OUTPUT PARAMETERS OF ZnO/CdS/ZnTe AND ZnO/CdS/ZnTe/P⁺-ZnTe SOLAR CELLS.

Solar cell	Voc (Volt)	Jsc (mA/cm ²)	FF (%)	η (%)	R _s (Ω.cm ²)
ZnO/CdS/ZnTe [12]	1.81	7.01	78.84	10	38.36
ZnO/CdS/ZnTe	1.795	8.75	78.16	12.28	31.87
ZnO/CdS/ZnTe/P ⁺ -ZnTe	1.81	9.35	79.05	13.37	31.43

Moreover, it is very known that series resistance R_s and shunt resistance R_{sh} affect the output parameters of solar cells. Because of series resistance, maximum achievable output power of a solar cell is decreased and this is reflected in the “softening” of its current-voltage characteristic in the fourth quadrant. In this sense, series resistance R_s of the simulated solar cells based on ZnTe thin films with and without P^+ -ZnTe back surface layer have been calculated and the obtained values are shown in table III. It is observed that R_s has been improved after the optimization of ZnO and CdS layers. Also, the insertion of P^+ -ZnTe back surface layer leads to a more significant decrease of R_s . The improvement of R_s is probably one of the main factors which has contributed to the enhancement of current and energy conversion efficiency.

The external quantum efficiency (EQE) has been calculated for ZnTe based solar cells with and without P^+ -ZnTe back surface layer and plotted in Figure 10. For ZnO/CdS/ZnTe solar cells, the spectral response in the long-wavelength region has decreased at the increase of back surface recombination velocity. However, it has exhibited a red shift and shown no dependence of back surface recombination velocity for ZnO/CdS/ZnTe/ P^+ -ZnTe solar cells. Also, the insertion of P^+ -ZnTe back surface layer has caused a slight extended absorption. Therefore, it can be concluded that the inserting of P^+ -ZnTe layer at the back surface of ZnTe active layer results in the inhibiting of back surface recombination loss and has enhanced the collection of more photogenerated carriers. Thus, the BSF effect has been produced and contributed to the improvement of the photocurrent and the conversion efficiency of ZnTe based solar cells.

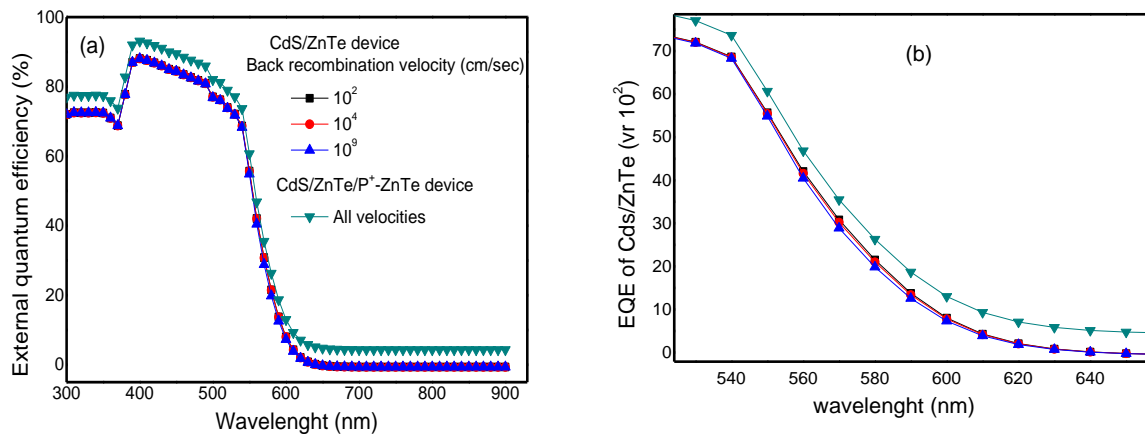


Figure 10: Spectral response of ZnO/CdS/ZnTe and ZnO/CdS/ZnTe/ P^+ -ZnTe solar cells for different back recombination velocities
(a): Total spectra (b): Zoomed spectra in 520-655 nm wavelength range.

IV. CONCLUSION

Numerical simulation by mean of SCAPS program has been performed on solar cells based on ZnTe thin films. Device structures with and without P^+ -ZnTe back surface layer have been proposed and

studied. Simulation calculations have showed that the highest power conversion efficiency (PCE) of the conventional ZnO/CdS/ZnTe solar cells was found to be 10 %, achieved with ZnTe, ZnO and CdS layer thicknesses closed to 2, 0.05 and 0.08 μm , respectively. When both ZnO and CdS layer thicknesses have been optimized to 0.03 μm , the optimal PCE of the cells has increased to 12.40 %. After inserting of a P⁺-ZnTe layer at the back surface of ZnTe absorber and optimization of ZnTe, ZnO, CdS and P⁺-ZnTe layer thicknesses to 0.5, 0.03, 0.03 and 0.1 μm , respectively the optimal PCE of ZnO/CdS/ZnTe/P⁺-ZnTe solar cells has raised to 13.37%. Furthermore, EQE curves have exhibited that the spectral response has decreased at the increase of back surface recombination rate for ZnO/CdS/ZnTe solar cells. However, they have showed no dependence of back surface recombination velocity and a red shift for ZnO/CdS/ZnTe/P⁺-ZnTe solar cells. From these results it is clear that a back surface field (BSF) effect has been produced due the P⁺-ZnTe layer inserted at the back surface of ZnTe active layer and it lead to inhibit the back surface recombination loss and contributed to improve the photocurrent and the conversion efficiency of ZnTe based solar cells. Finally, the produced BSF effect has caused a slight extended absorption of ZnTe based solar cells.

ACKNOWLEDGMENTS

This work was supported by Ministerio de Economía y Competitividad (ENE2016-77798-C4-2-R) and Generalitat valenciana (Prometeus 2014/044).

REFERENCES

- [1] J. Britt, C. Ferekides, *Appl. Phys. Lett.* 62 (1993) 2851.
- [2] N. Amin, T. Isaka, T. Okamoto, A. Yamada, M. Konagai, *Jpn. J. Appl. Phys.* 38 (8) (1999) 4666.
- [3] N. Amin, T. Isaka, A. Yamada, M. Konagai, *Sol. Energy Matter. Sol. Cells* 67 (2001) 195.
- [4] R.J. Schwartz, G.B. Turner, *Proc. IEEE* (1987) 0019.
- [5] S.M. Durbin, J.L. Gray, *Proc. IEEE* (1991) 0181.
- [6] A. Kaneta, S. Adachi, *Journal Physics D: Applied Physics* 33, 901 (2000).
- [7] A. Pistone, A.S. Arico, P.L. Antonucci, D. Silvestro, V. Antonucci, *Sol. Energy Mater. and Sol. Cells* 53, 255 (1998).
- [8] J. M. Pawlikowski, « Comments on the determination of the absorption coefficient of thin semiconductor films », *Thin Solid Films*, vol. 127, no 1, p. 29–38, 1985.
- [9] J. D. Dow, R.-D. Hong, S. Klemm, S. Y. Ren, M.-H. Tsai, O. F. Sankey and R. V. Kasowski, *Phys. Rev. B (Condensed Matter)* 43 (1991) 5396.
- [10] C. Soykan, S. Ozdemir Kart, T. Cagin, *Archives of Materials Science and Engineering*, 46(2), (2010) 115-119.

- [11] G. Mandel, "Self-compensation limited conductivity in binary semiconductors". *Phys. Rev.* 134 (1964) A1073
- [12] O. Skhouni, A. El Manouni, B. Marí, *Eur. Phys. J. Appl. Phys.* 74 (2), 24602 (2016).
- [13] Alex Niemegeers, Marc Burgelman, and Koen Decock (SCAPS Manual, 2014), University of Gent.
- [14] S. Fonash, *Solar Cell Device Physics*, 2nd ed. (Elsevier, 2012).
- [15] D. Verity, F. J. Bryant, C. G. Scott, et D. Shaw, « Deep level transient spectroscopy of hole traps in Zn-annealed ZnTe », *Solid State Commun.*, vol. 46, no 11, p. 795-798, juin 1983.
- [16] O. Skhouni, A. El Manouni, M. Mollar, R. Schrebler, B. Marí, *Thin Solid Films* 564, 195 (2014).
- [17] W. Shockley, W.T. Read, *Phy. Rev.* 87, 835 (1952).
- [18] Z. Fan, J.G. Lu, *J. of Nanosci. and Nanotech.*, 5 (10), 1561 (2005).